RHESSI 15 - Narukage et al. (2014) ApJ, 787, 125

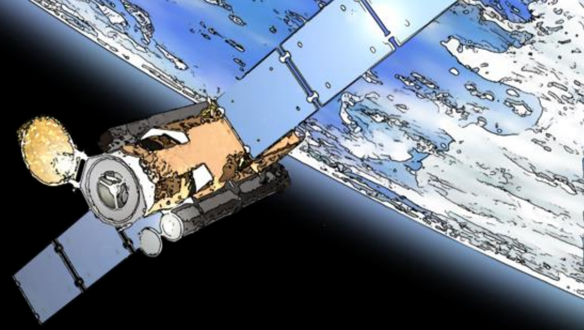

Evidence of Electron Acceleration around the Reconnection X-point in a Solar Flare

N. Narukage (NAOJ)
M. Shimojo (NAOJ), T. Sakao (ISAS/JAXA)

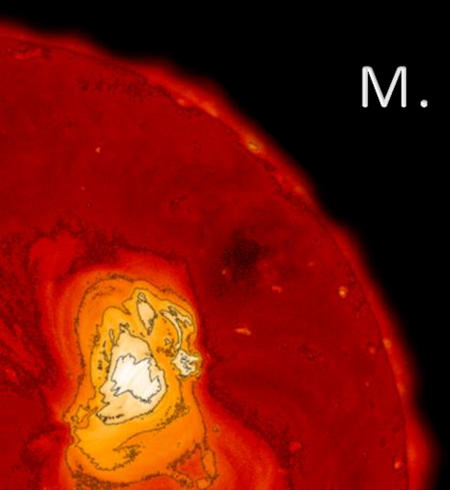

Outline

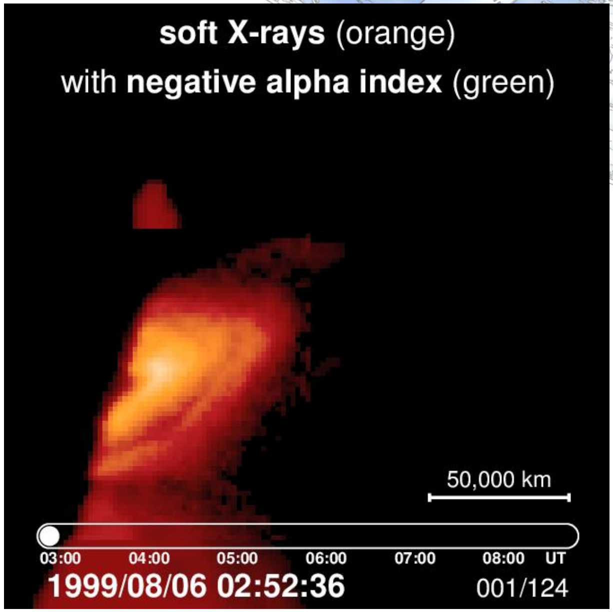

- Introduction: Particle acceleration site in solar flares
- Discovery of non-thermal signal around the X-point
  - Observation data
  - Identification of the X-point in soft X-rays
  - Detection of non-thermal signal in microwave
  - Time evolution of the non-thermal component
- Discussion: The energetic non-thermal electrons are accelerated around the X-point.
- Energy budget around the X-point in a solar flare (preliminary result)

Introduction

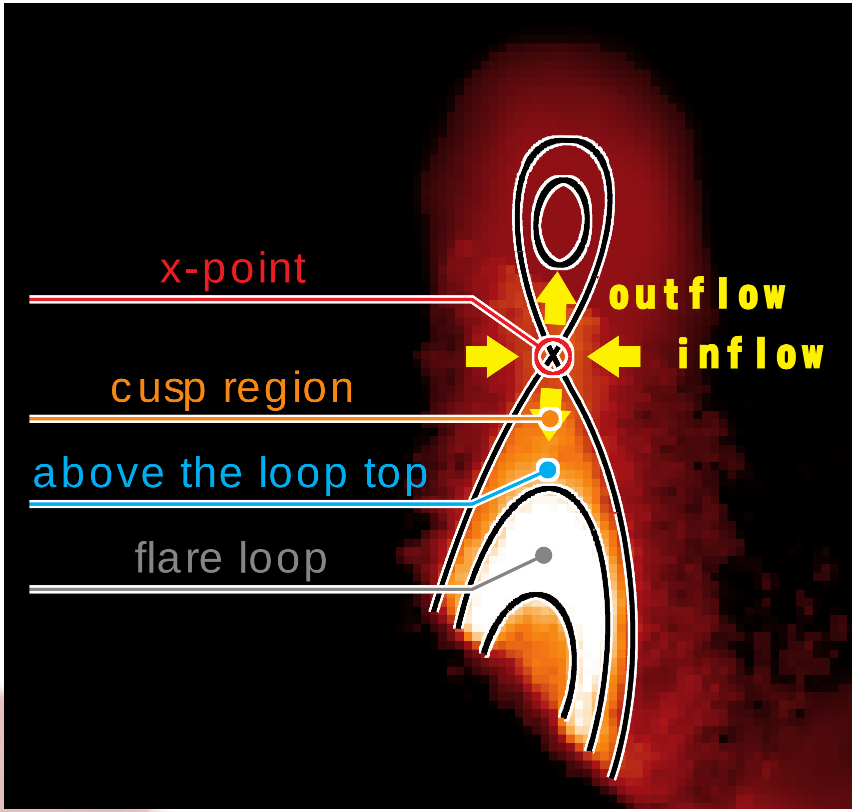

- Particle acceleration site was puzzle.
- Candidate of the acceleration site
  - **Closed magnetic loop**
    - Fletcher & Hudson (2008)
  - **Above-the-loop-top**
    - Tsuneta & Naito (1998)
  - **Cusp region**
    - Somov & Kosugi (1997)
  - **X-Point/Current Sheet**
    - Litvinenko (1996)
    - Pritchett (2006)
    - Drake et al. (2006)
    - Oka et al. (2010)

Observation datasets

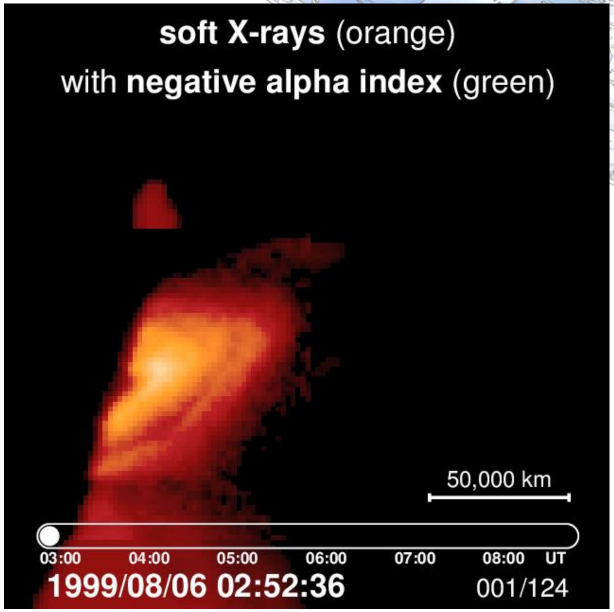

- Date : 1999/08/06 4:34 (UT) ～
- Flare site : AR 8645 (S28W91)
- Flare class : Unknown
  (GOES X-ray light curve is almost flat at ~C6 level, probably because this flare was not large enough in soft X-ray flux against the other eight active regions simultaneously located on the solar disk.)
- Data sets
  - Soft X-rays : ***Yohkoh***/SXT
  - Microwave : Nobeyama RadioHeliograph (17GHz and 34GHz)
  - No Hard X-ray (Yohkoh/HXT) data

National Astronomical Observatory of Japan

Identification of X-point in soft X-rays (Yohkoh/SXT)

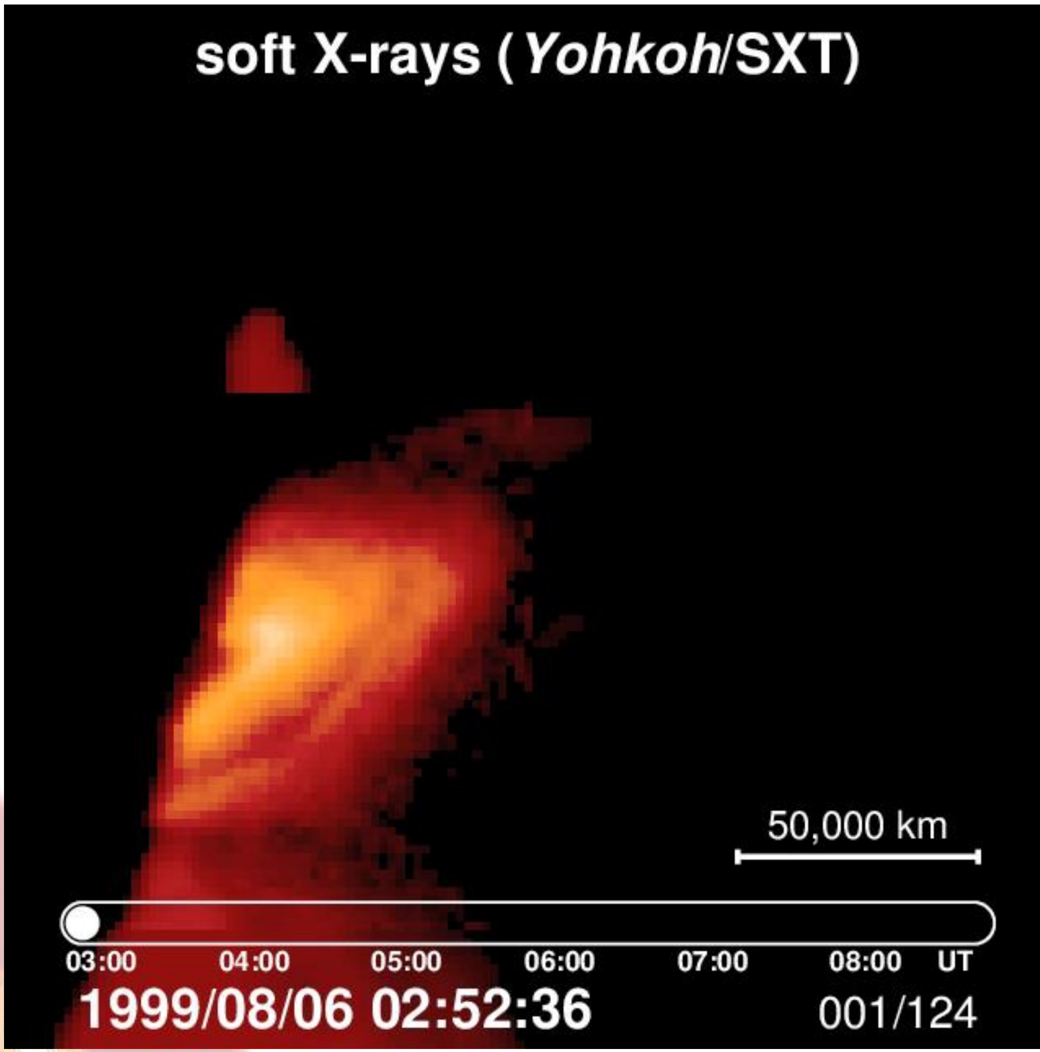

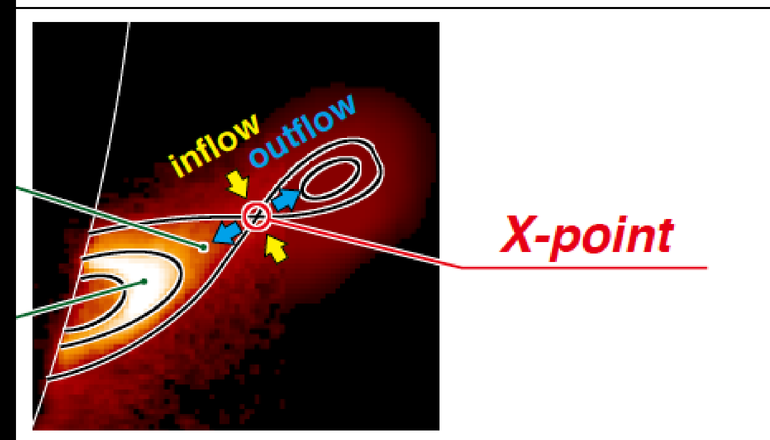

RHESSI 15 - Narukage et al. (2014) ApJ, 787, 125

Identification of X-point in soft X-rays (Yohkoh/SXT)

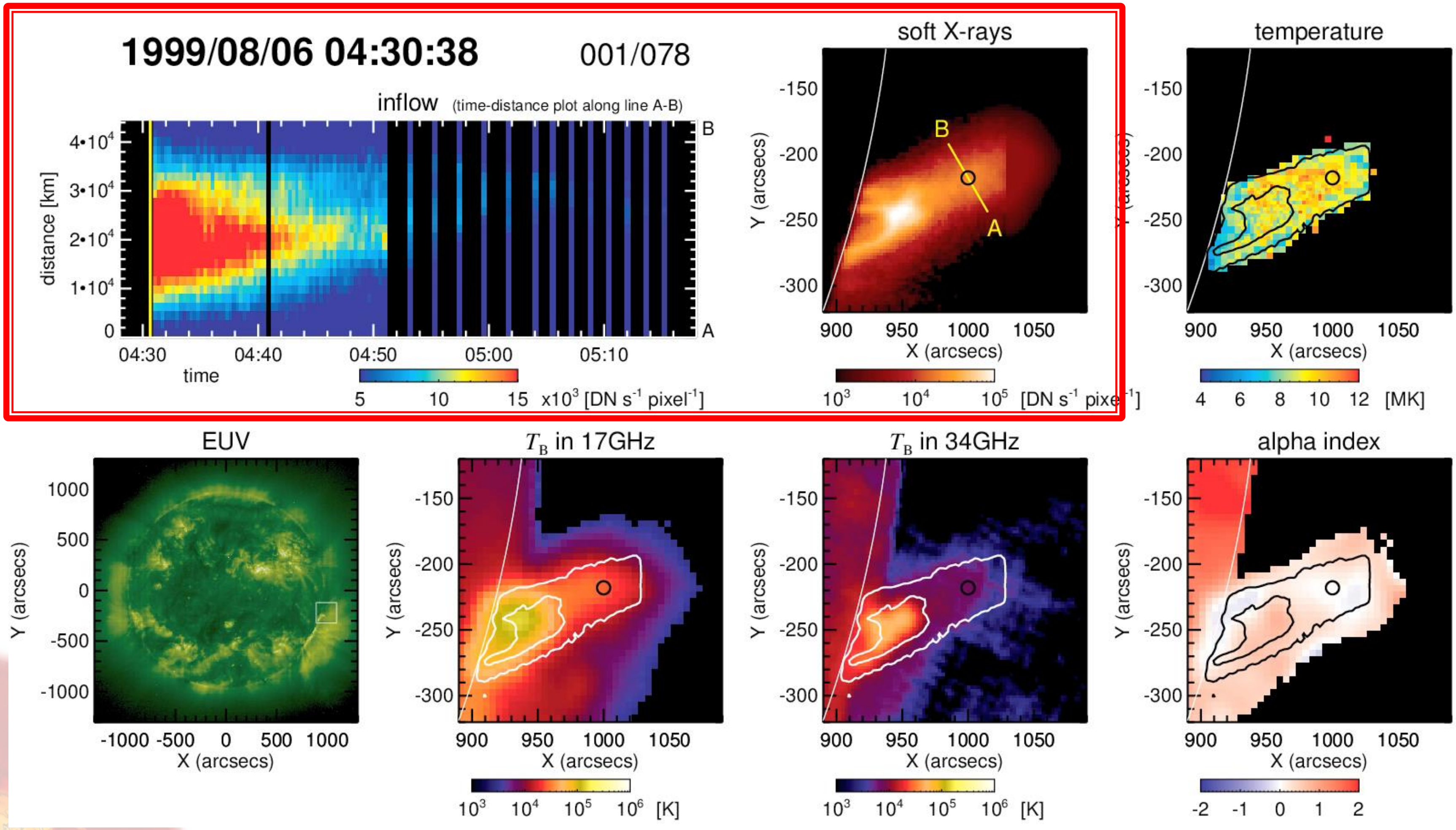

RHESSI 15 - Narukage et al. (2014) ApJ, 787, 125

Inflow & X-ray intensity from the loop

Inflow velocity : ~ 16.3 km/s

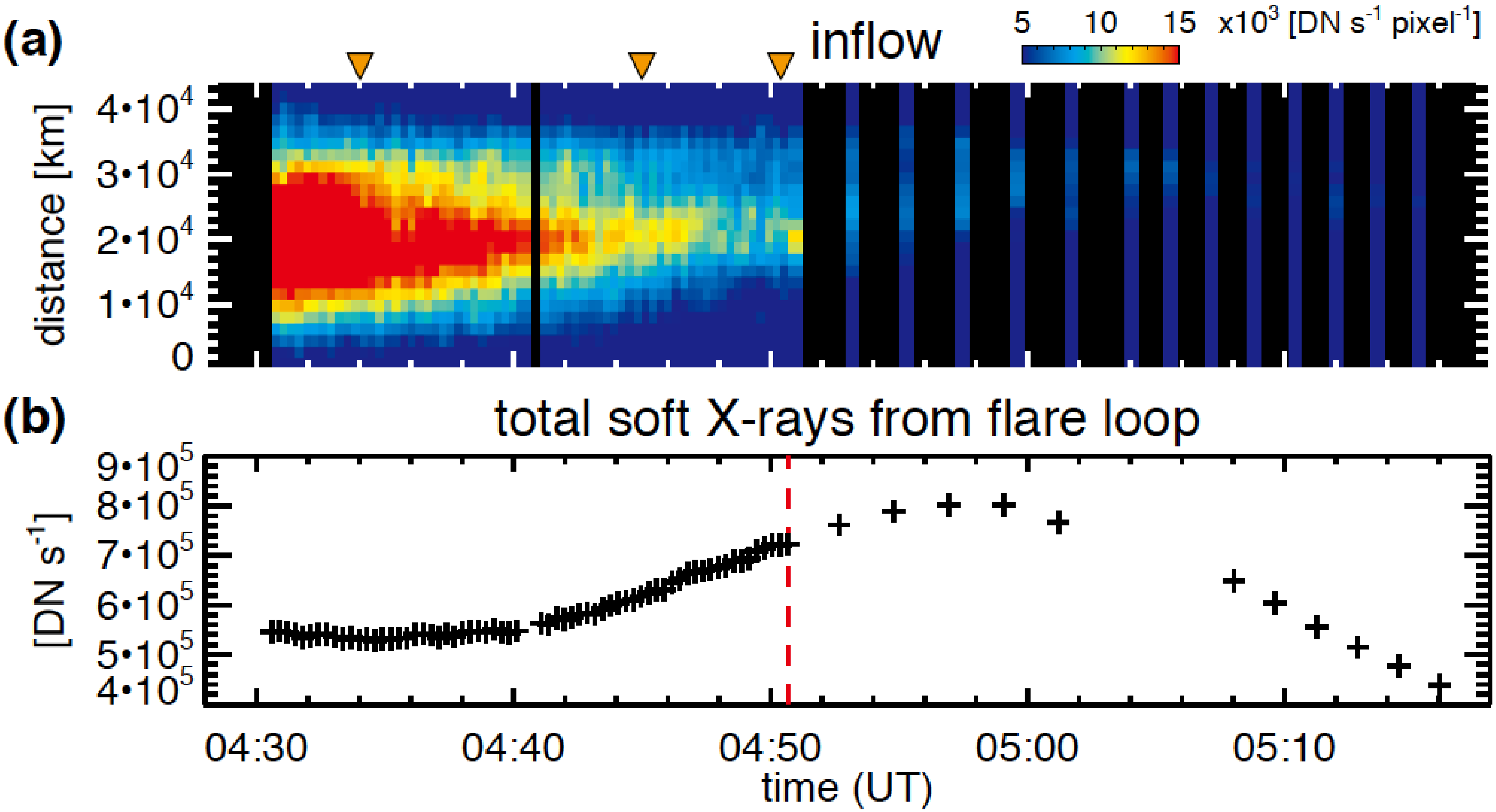

RHESSI 15 - Narukage et al. (2014) ApJ, 787, 125

Identification of X-point in soft X-rays（Yohkoh/SXT）

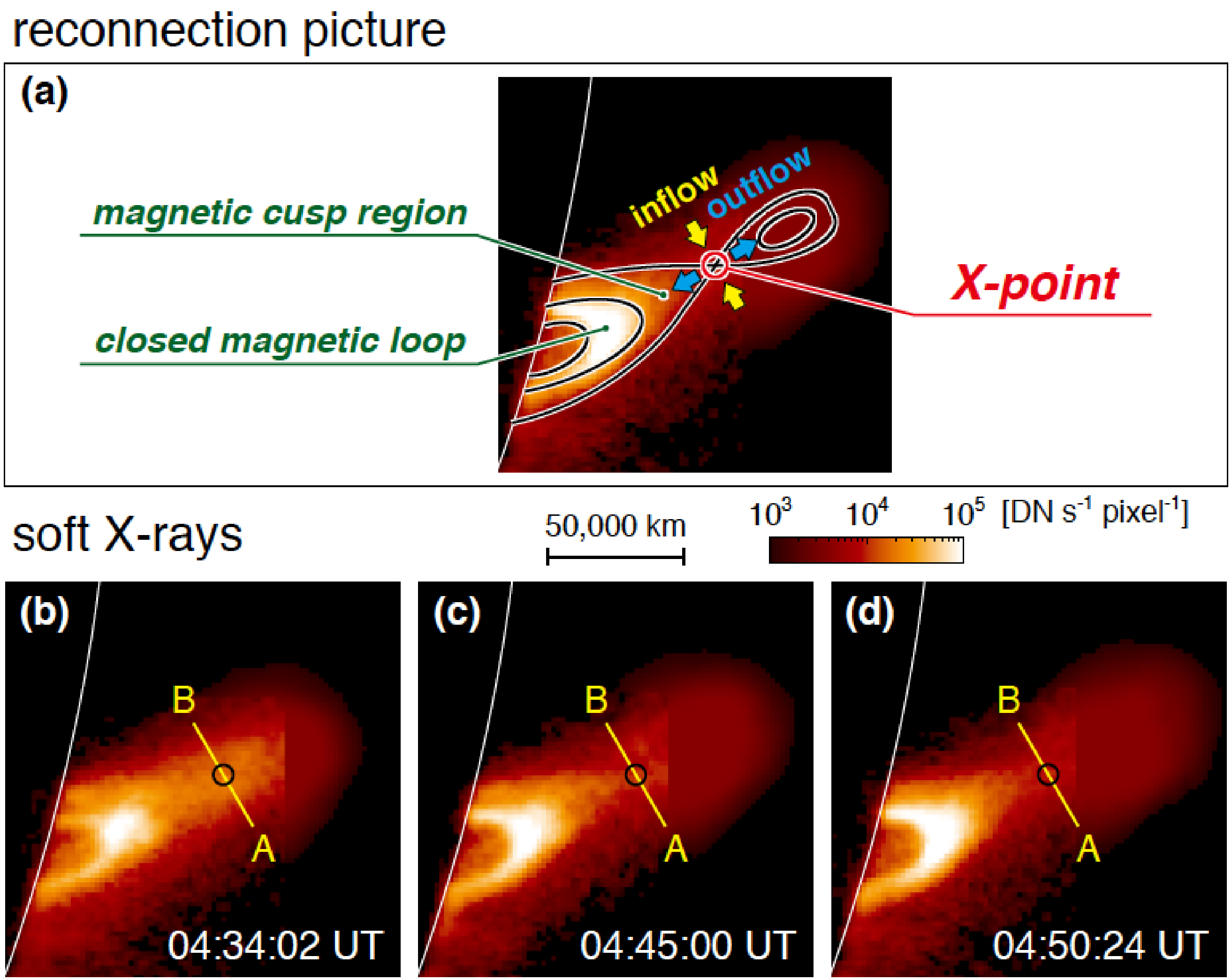

RHESSI 15 - Narukage et al. (2014) ApJ, 787, 125

Detection of non-thermal signal in microwave

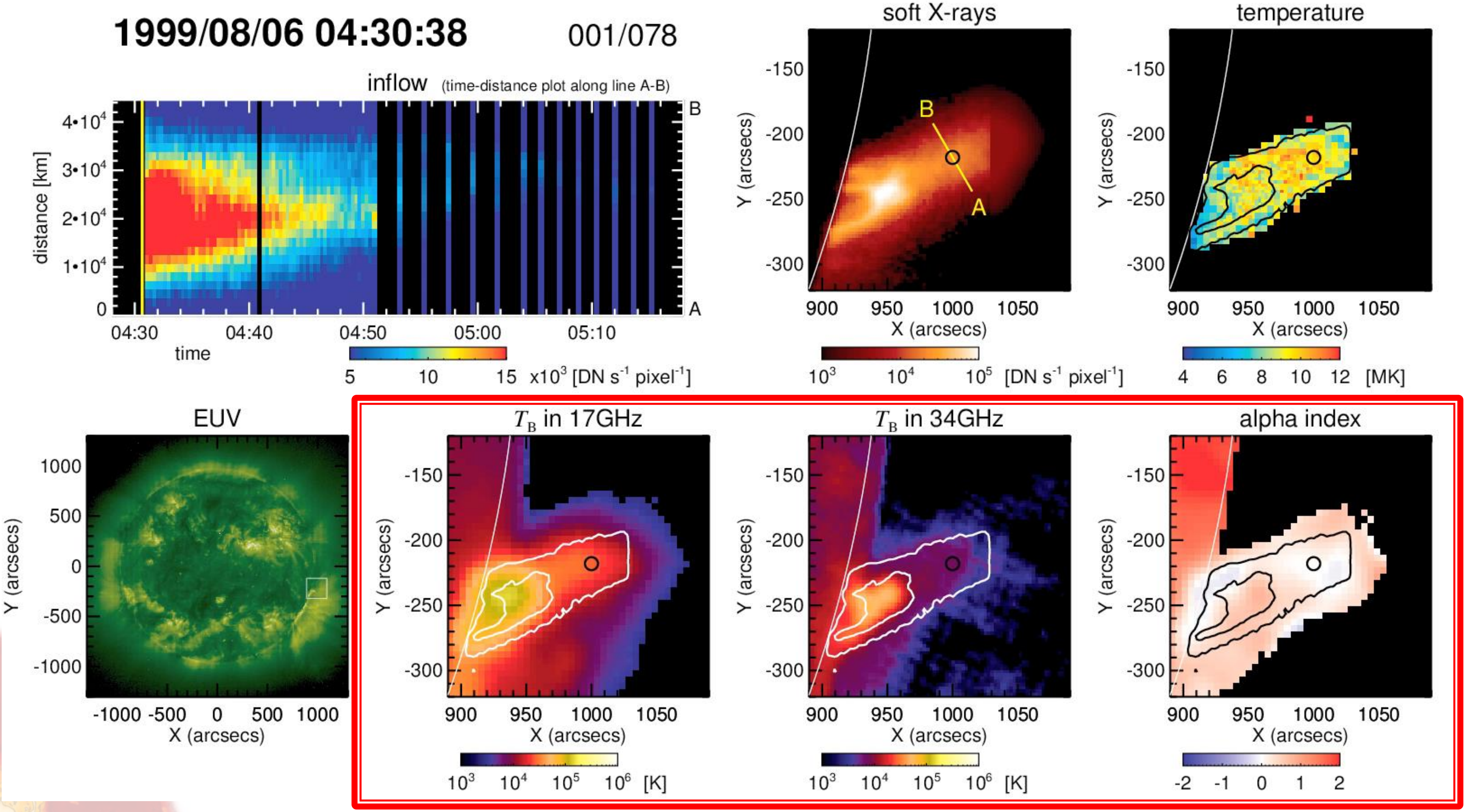

RHESSI 15 - Narukage et al. (2014) ApJ, 787, 125

α index (Dulk 1985)

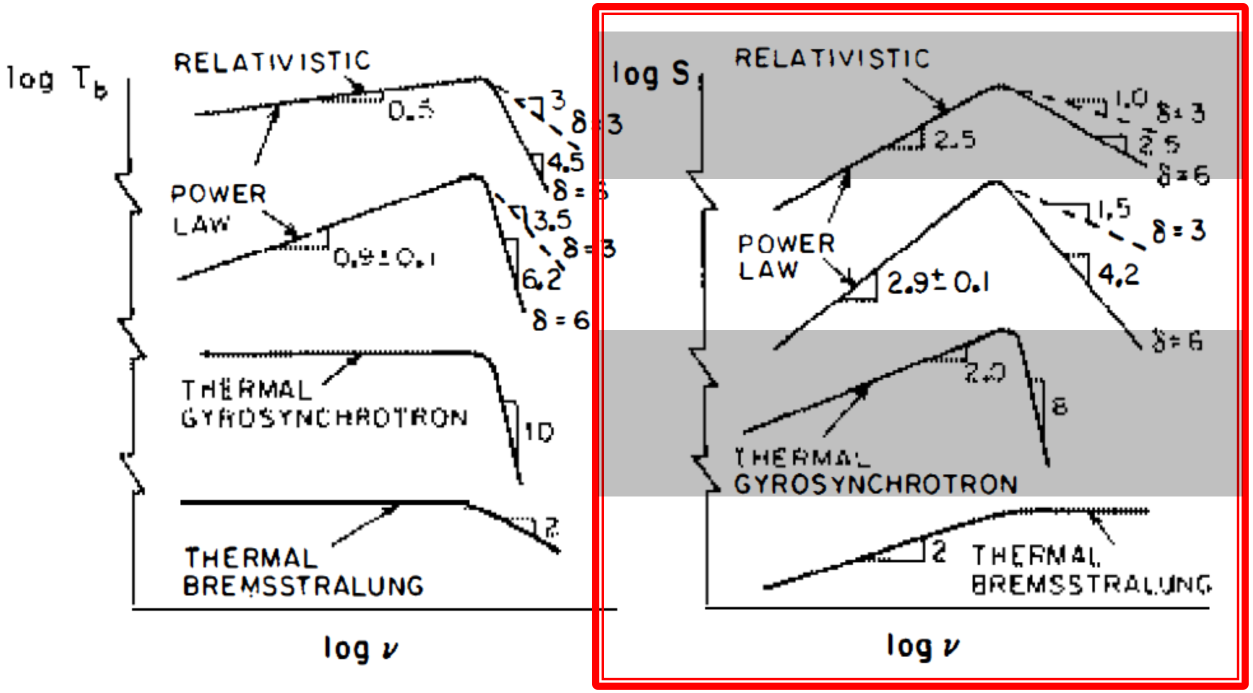

Relativistic case

Non-thermal

Above sun spots

Thermal

Emission mechanism	alpha index	
	Optically thick	Optically thin
Non-thermal gyro-syncrotoron from mildly-relativistic electrons	$+2.9 \pm 0.1$	-1.5 for $\delta_\mu = 3$[a] -4.2 for $\delta_\mu = 6$
Thermal gyro-syncrotoron (Gyro-resonance)	$+2$	-8
Thermal Bremsstrahlung	$+2$	0

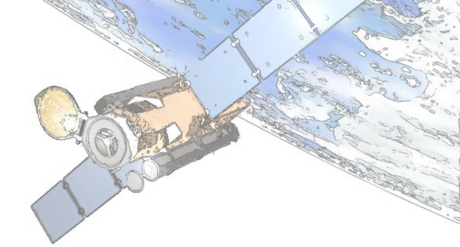

Detection of non-thermal signal in microwave

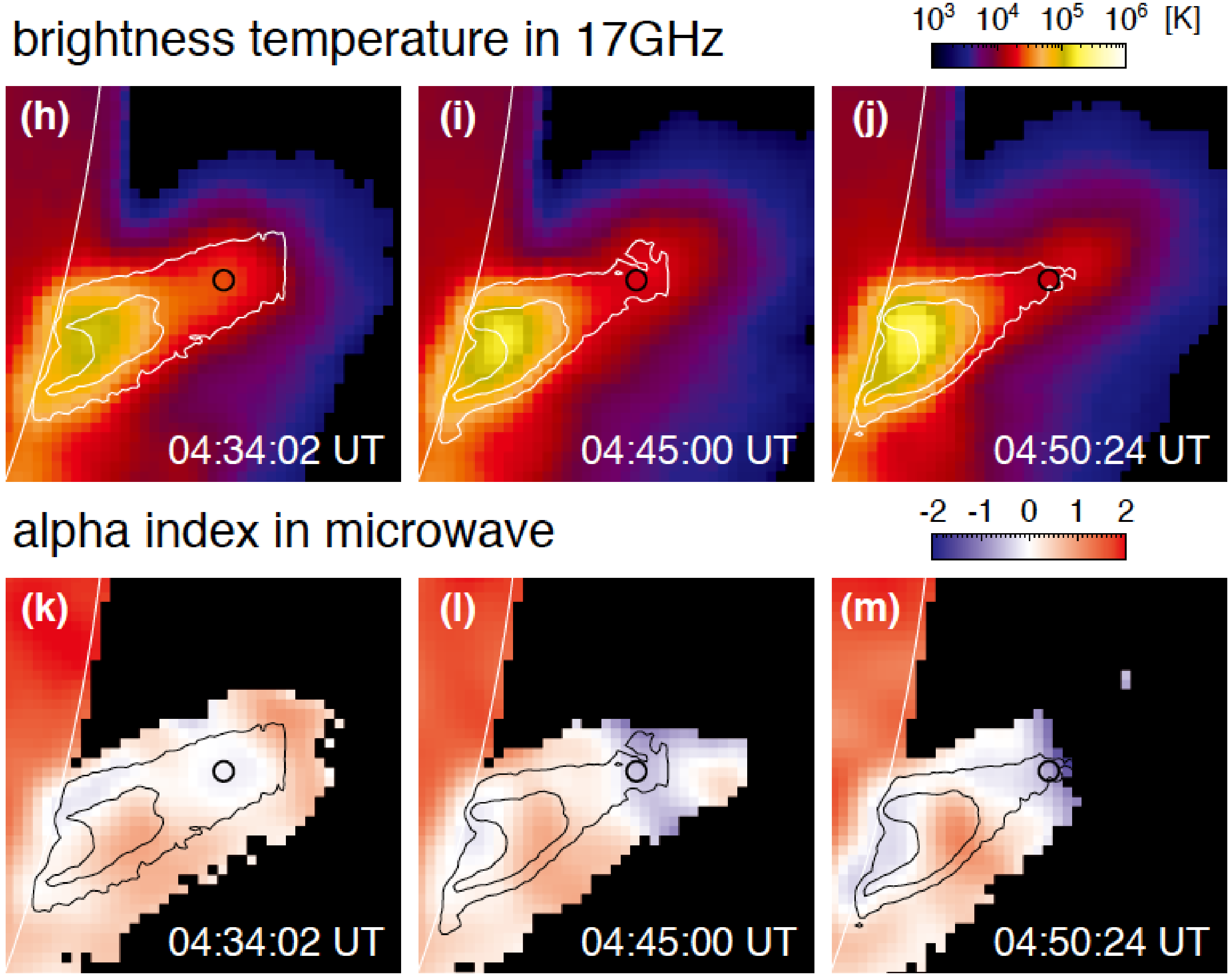

RHESSI 15 - Narukage et al. (2014) ApJ, 787, 125

Time evolution of α index around the X-point

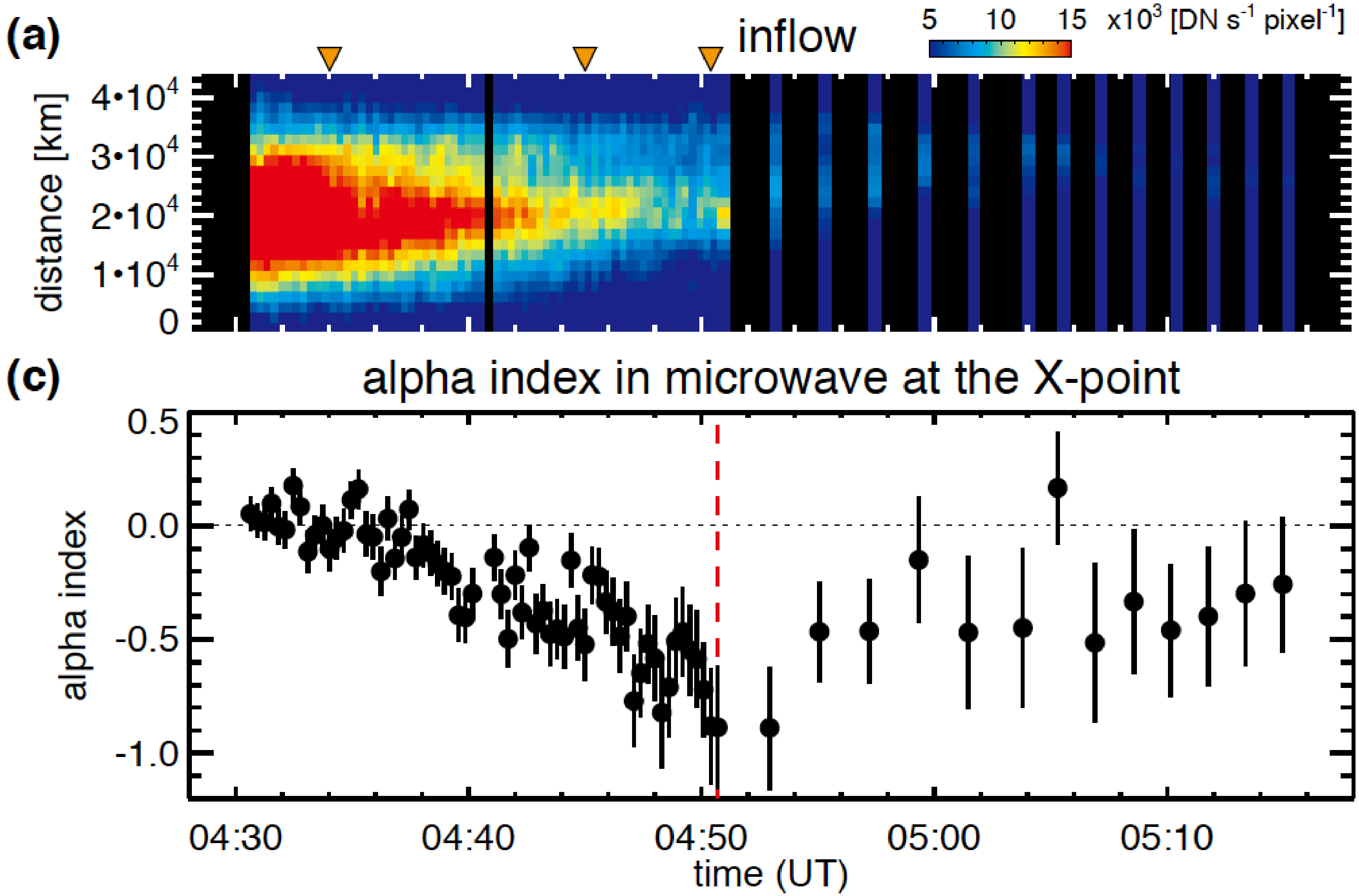

RHESSI 15 - Narukage et al. (2014) ApJ, 787, 125

Time evolution of α index around the X-point

- This negative α-index suggests the existence of non-thermal electrons.
- However, this α-index is a net index generated by both of co-existing thermal and non-thermal electrons.

➔ For more confirmation of the existence of non-thermal electrons, we will remove the thermal components (see following slides).

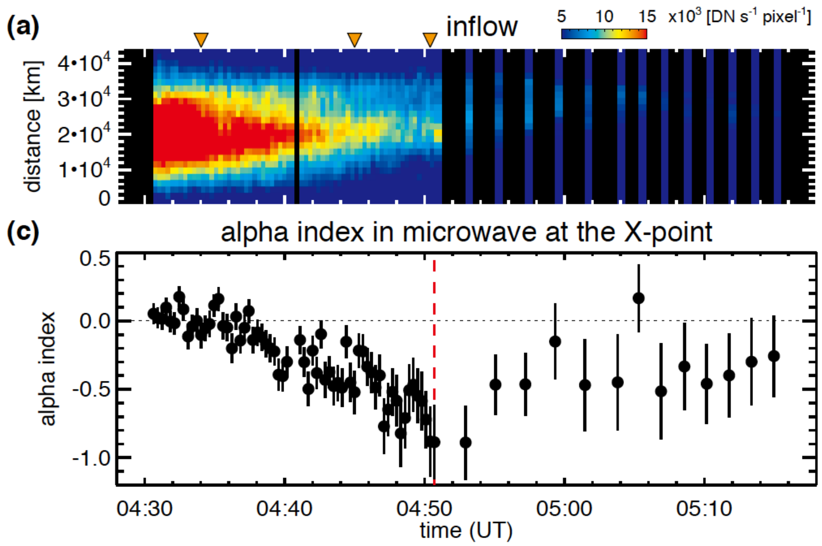

Estimate of the thermal component

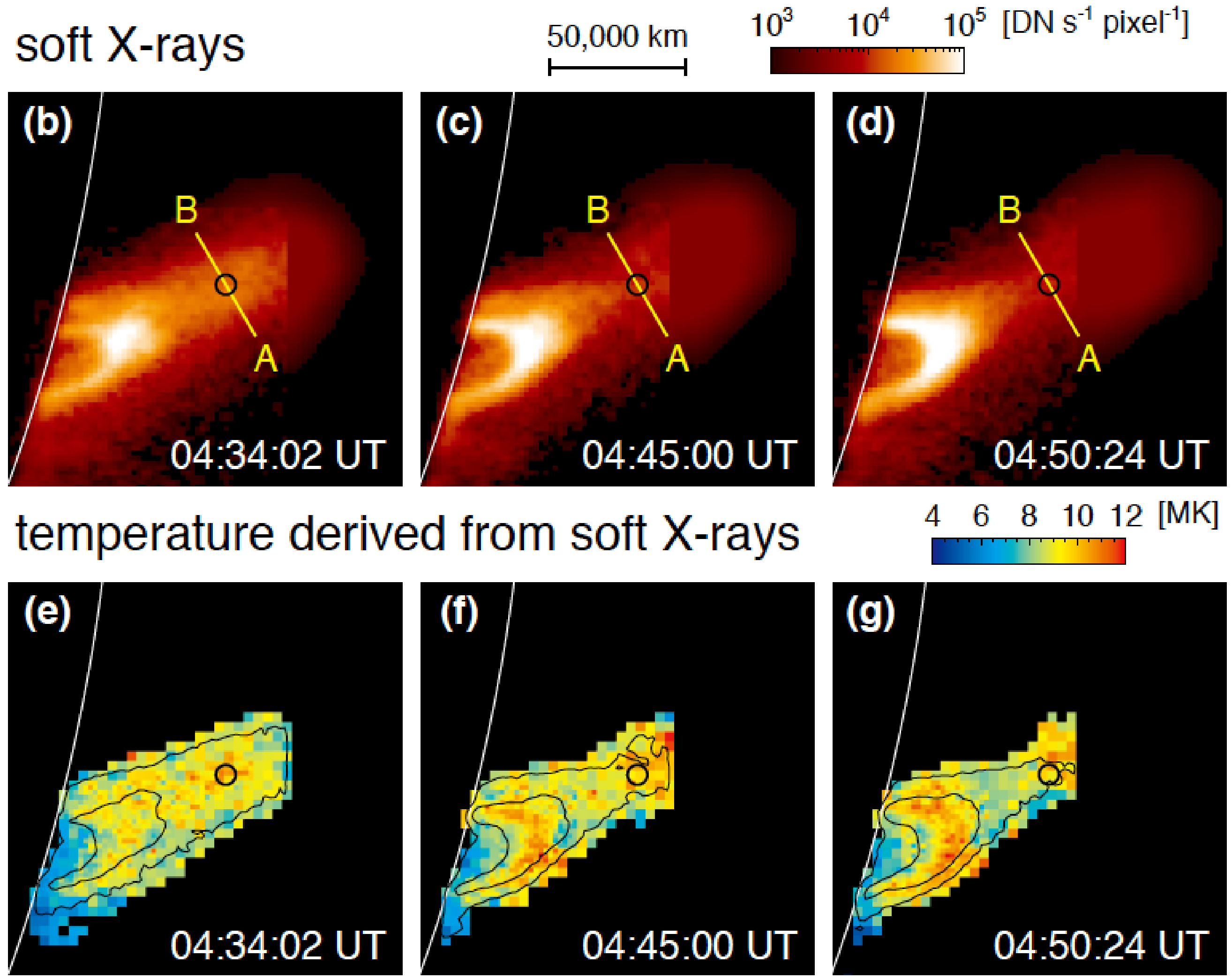

RHESSI 15 - Narukage et al. (2014) ApJ, 787, 125

Time evolution of the thermal component (T and EM) around the X-point

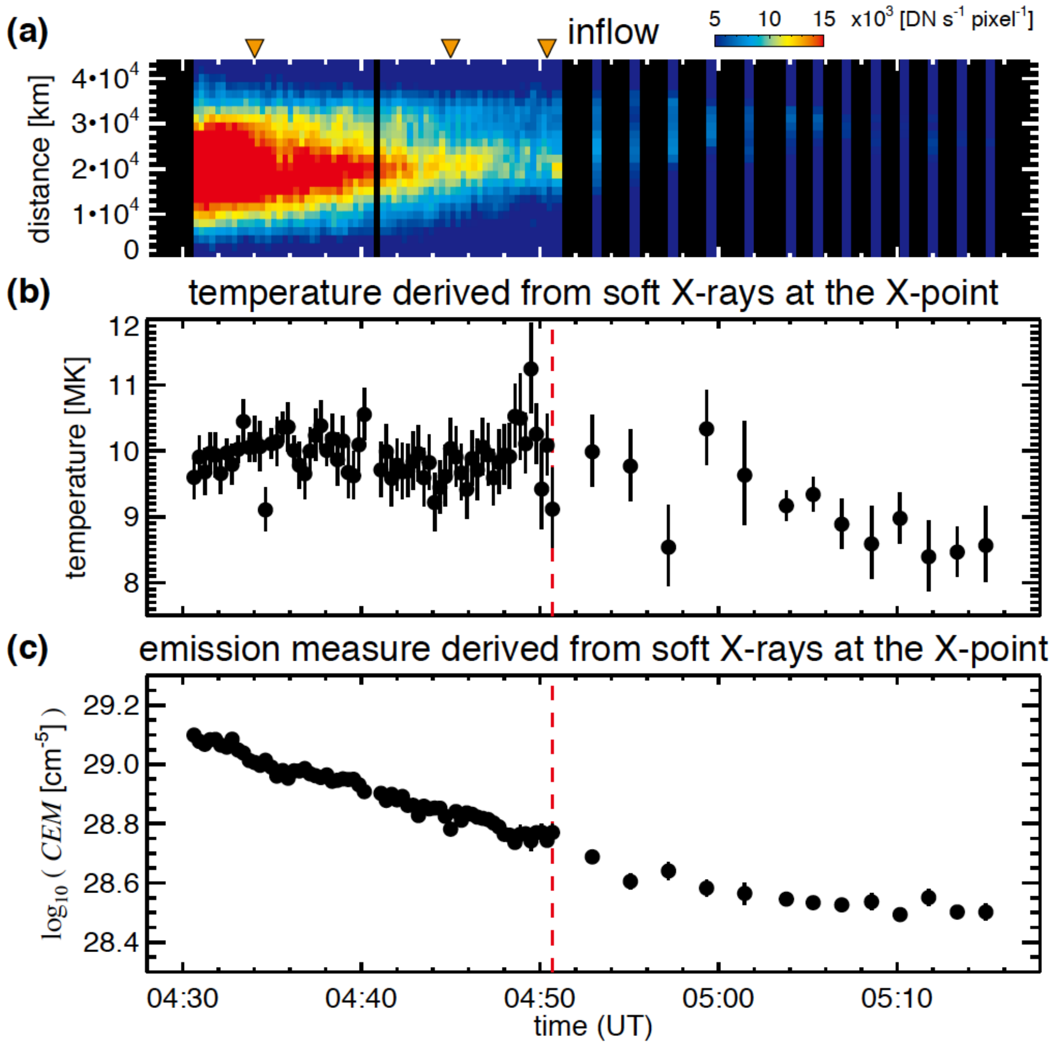

RHESSI 15 - Narukage et al. (2014) ApJ, 787, 125

Estimate of thermal Bremsstrahlung component in radio 17 GHz (Dulk 1985)

- Absorption coefficient

$$\kappa_\nu \approx \sum_i \frac{1}{3c}\left(\frac{2}{\pi}\right)^{1/2} \frac{\nu_p^2}{\nu^2} \frac{4\pi Z_i^2 n_i e^4}{m^{1/2}(kT)^{3/2}} \frac{\pi}{\sqrt{3}} G(T,\nu) \qquad 20.$$

$$\approx 9.78 \times 10^{-3} \frac{n_e}{\nu^2 T^{3/2}} \sum_i Z_i^2 n_i$$

$$\times \begin{cases} 18.2 + \ln T^{3/2} - \ln \nu & (T < 2 \times 10^5\ \mathrm{K}) \\ 24.5 + \ln T - \ln \nu & (T > 2 \times 10^5\ \mathrm{K}). \end{cases}$$

- Emissivity (Kirchhoff's Law)

$$\eta_\nu = \kappa_\nu k T \nu^2/c^2\ \mathrm{erg\ cm^{-3}\ s^{-1}\ Hz^{-1}\ sr^{-1}}. \qquad 7.$$

- Brightness temperature

$$T_b = T_{\mathrm{eff}} \qquad (\text{if } \tau_\nu \gg 1) \qquad 12.$$

$$= T_{\mathrm{eff}}\tau_\nu = (c^2/k\nu^2)\eta_\nu L \qquad (\text{if } \tau_\nu \ll 1), \qquad 13.$$

Time evolution of the thermal component in 17GHz around the X-point

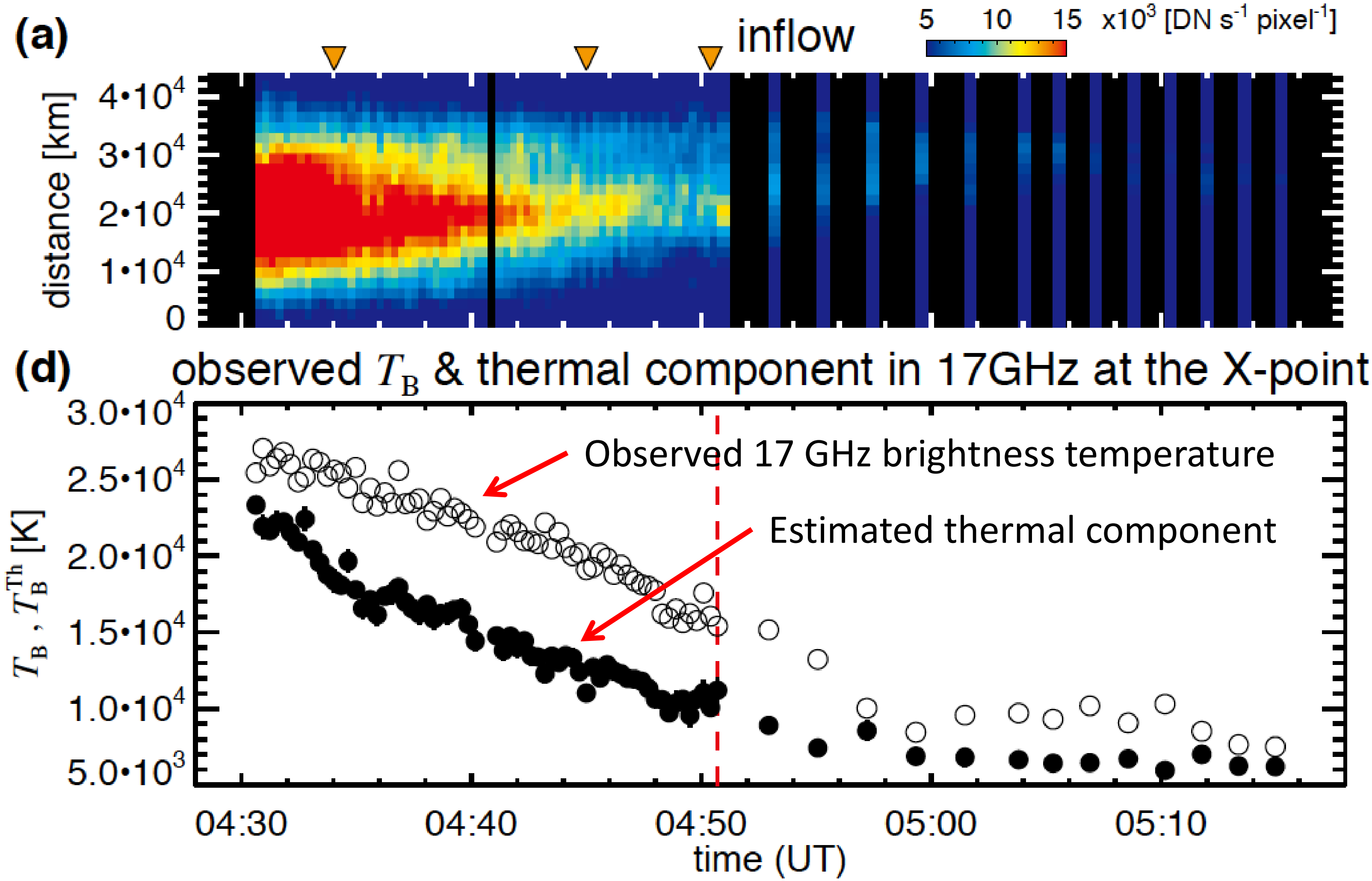

RHESSI 15 - Narukage et al. (2014) ApJ, 787, 125

Time evolution of the non-thermal component in 17GHz around the X-point

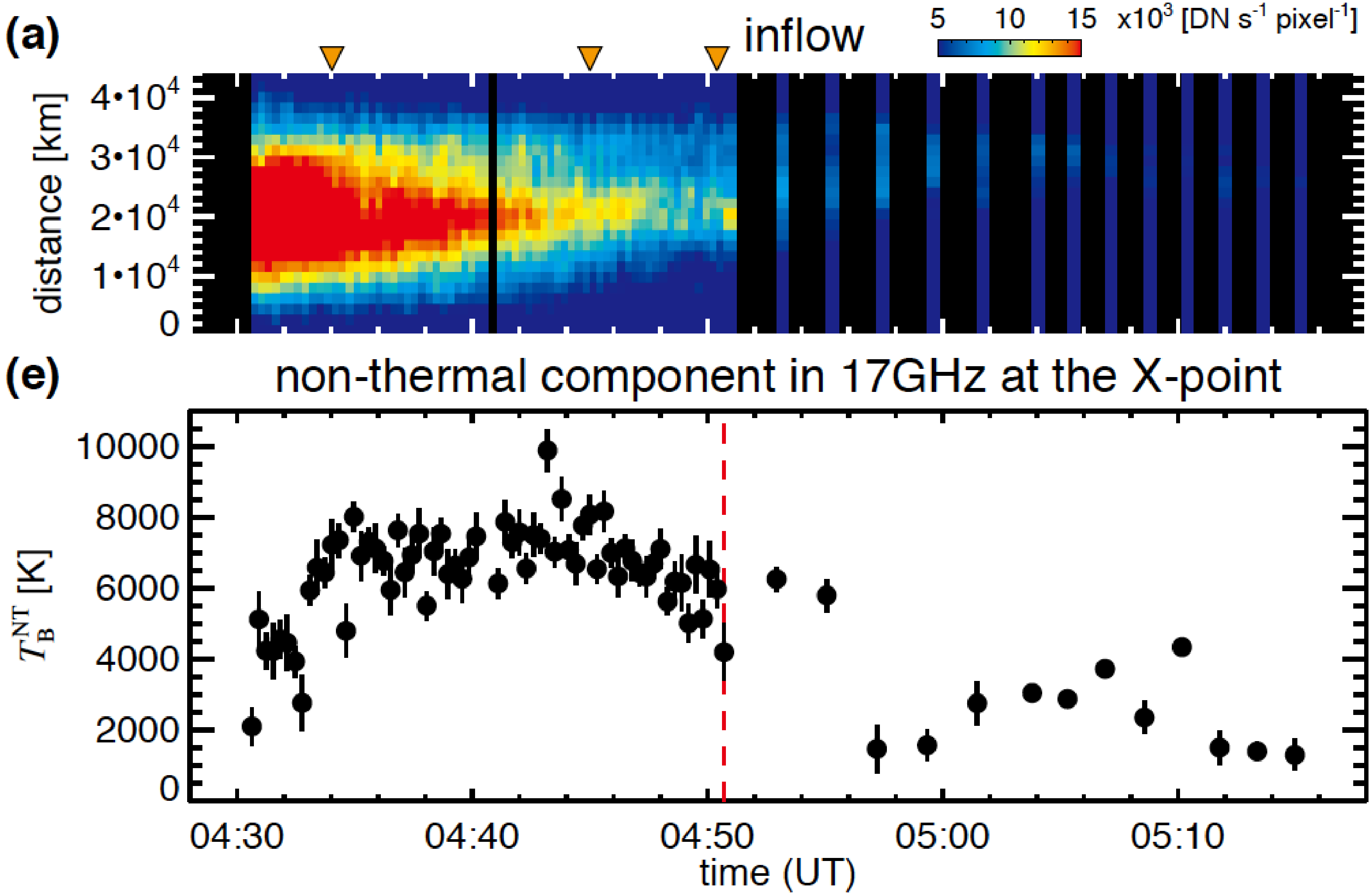

RHESSI 15 - Narukage et al. (2014) ApJ, 787, 125

Non-thermal component overlaid on SXR image

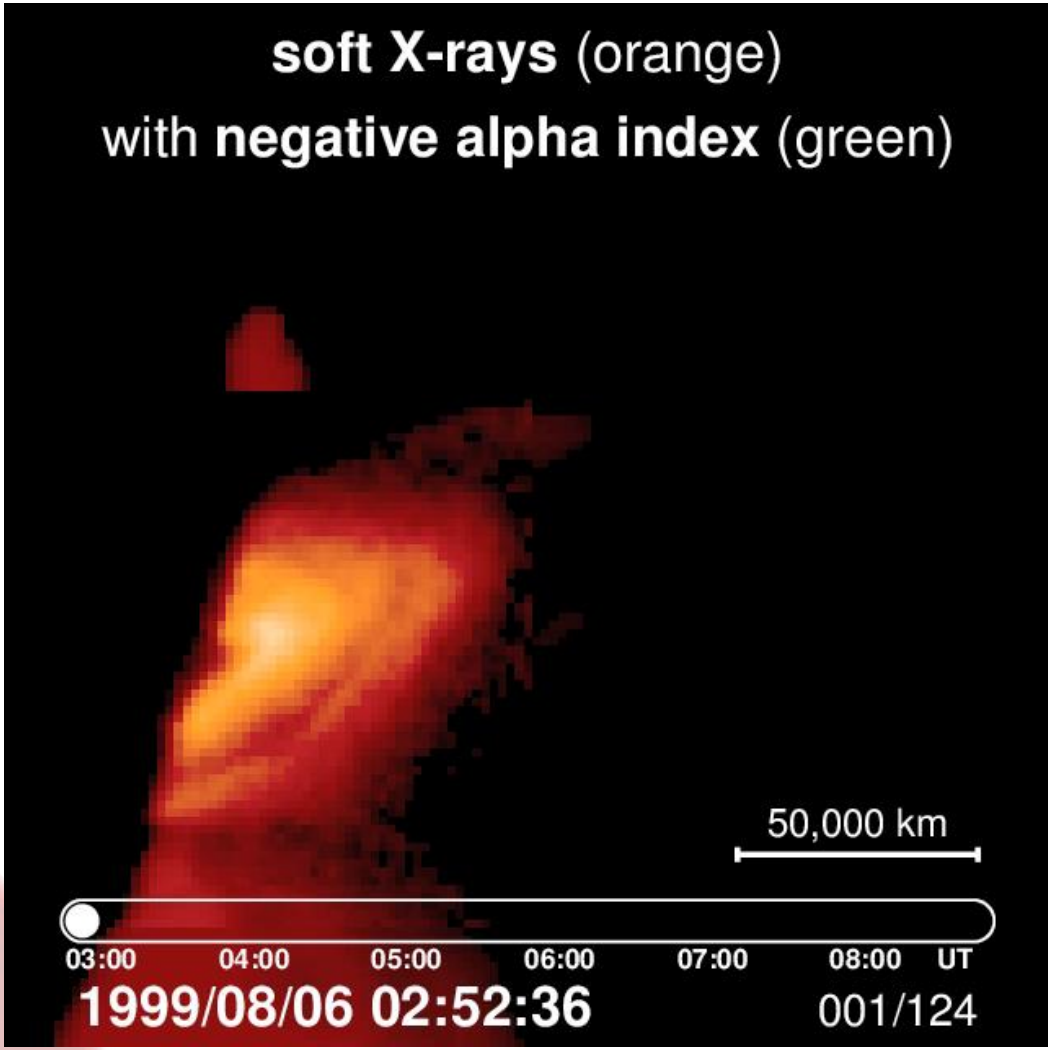

Narukage et al. (2014)
ApJ, 787, 125

Summary of the observations

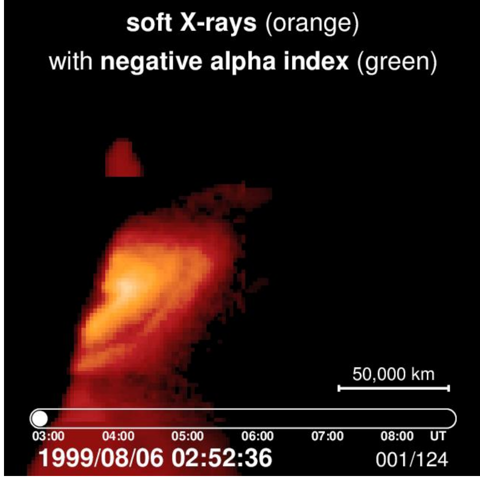

- Identified the location of X-point with SXR data.
- Discovered the non-thermal signal around the X-point with microwave imaging spectroscopic data.
- Such non-thermal signal increased with the progress of the inflow, and decreased after the end of inflow (after the plasmoid ejection).
  ➔ This suggests that the non-thermal signal has well consistency with the reconnection .

- Hot thermal component (~ 10MK) coexisted around the X-point together with the non-thermal component.
- Reconnection rate of this flare is ~ 0.017.

Discussion

- On the basis the reconnection theory, the bidirectional outflow carries plasma particles and magnetic fields away from the X-point towards the bright soft X-ray loop and in the opposite direction.
- Assuming the presence of the expected reconnection outflow, it would be reasonable to conclude that the energetic non-thermal electrons are supplied from, namely, accelerated at, the region around the X-point.

➔ Around the X-point is an initial acceleration site.

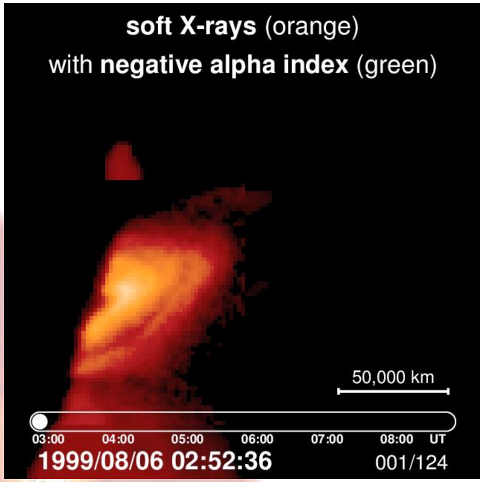

reconnection picture

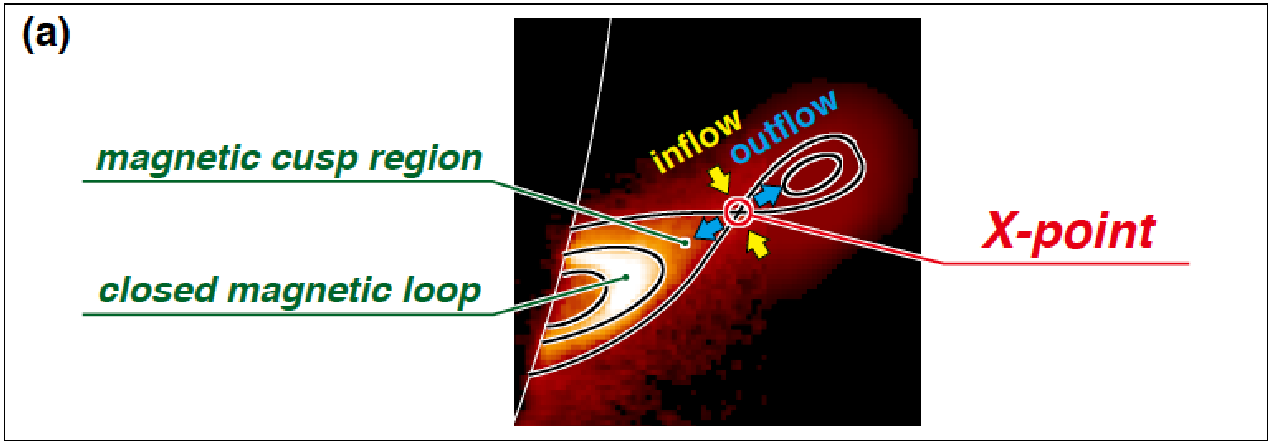

Future plan

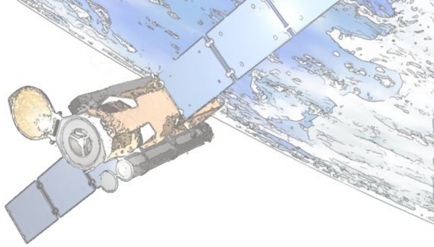

- We should increase the number of events using the data sets taken
  - with Yohkoh/SXT, Hinode/XRT, SDO/AIA, *Yohkoh/HXT, RHESSI* and **NoRH** (data survey).
  - with Hinode/XRT, SDO/AIA, *RHESSI* and **ALMA** **(Atacama Large Millimeter/submillimeter Array)** (new observation).

C-1

HIGH-ENERGY ELECTRONS IN MAGNETIC RECONNECTION **2016.1.00070.S**

ABSTRACT

Particle acceleration is a ubiquitous phenomenon in almost all space and cosmic plasmas, yet the details of the mechanisms driving the particle acceleration remain poorly constrained observationally. The Sun, due to its proximity and dynamics, is arguably the best astrophysical laboratory, but even there the problem of particle acceleration remains a mystery and represents a great challenge both theoretically and observationally. Our prior work with microwave imaging data in combination with X-ray data suggests that acceleration regions are localized around the point of ongoing magnetic reconnection. However, the available observations never had the spatial resolution and image fidelity needed to resolve the acceleration region and study its spatial structure and time evolution. Here we propose to make observations of nonthermal emission from microflares to detect and quantify the particle acceleration at the Sun with the level of detail not yet available before. To maximize the chances to clearly isolate the nonthermal emission from a microflare, we propose to make observations above the limb, where the background optically thin coronal thermal emission is relatively weak.

PI NAME:	Masumi Shimojo	SCIENCE CATEGORY:	Stellar Evolution and the Sun

RHESSI 15 - Narukage et al. (2014) ApJ, 787, 125

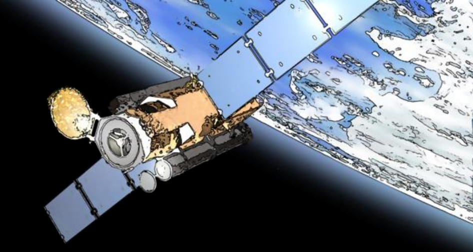

Energy budget around the reconnection X-point in a solar flare

Preliminary result

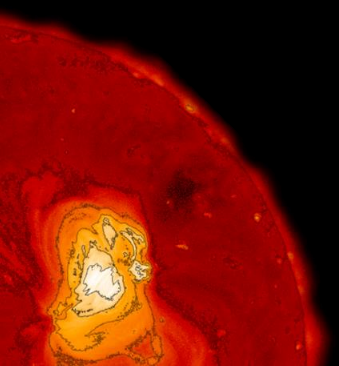

RHESSI 15 - Narukage et al. (2014) ApJ, 787, 125

Energy budget around the X-point in a solar flare

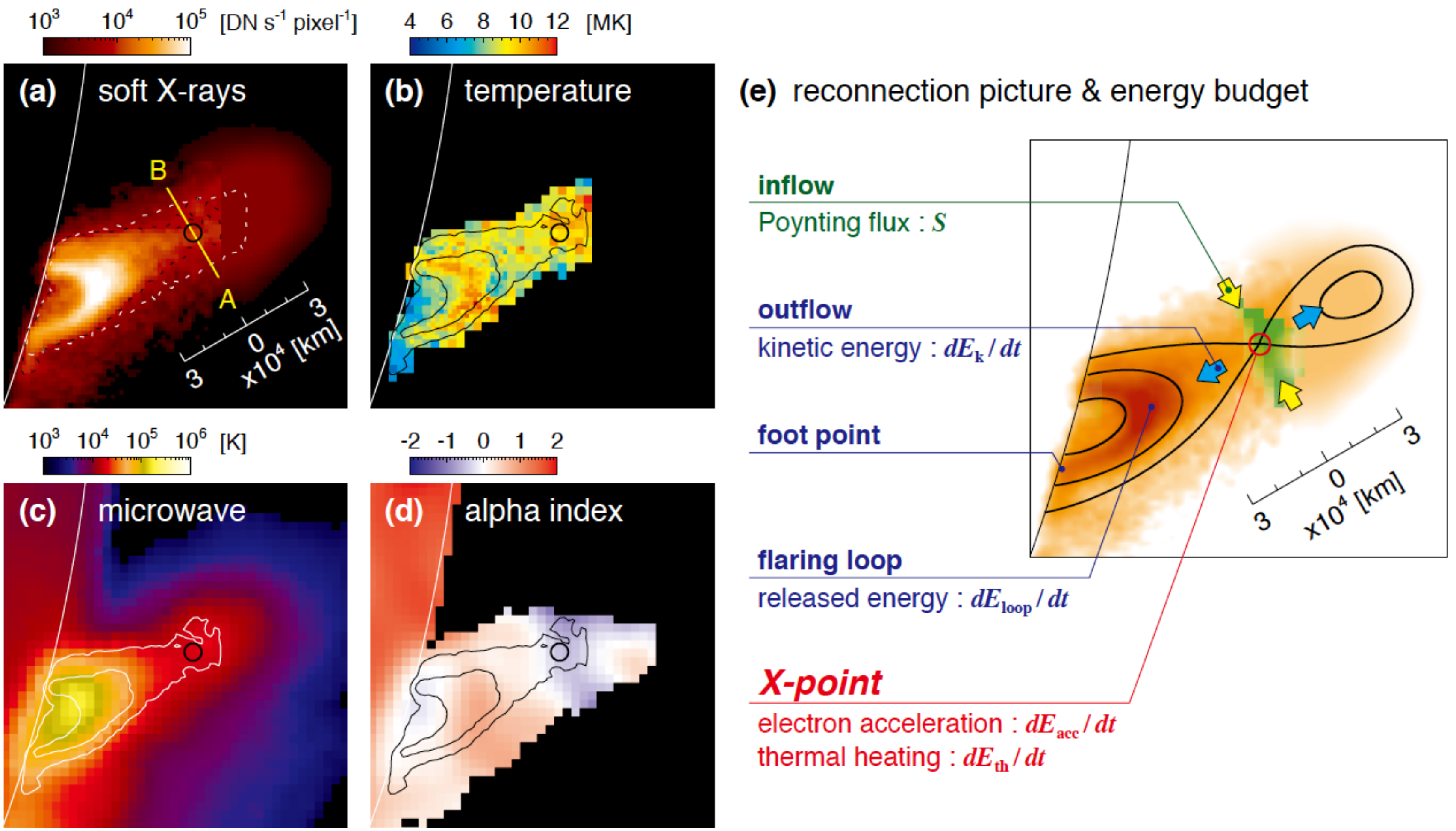

RHESSI 15 - Narukage et al. (2014) ApJ, 787, 125

Energy budget around the X-point in a solar flare (preliminary result)

Table 2: Energy budget around the reconnection X-point.

Input energy		
Poynting flux carried by inflow	$E_{\mathrm{S}} = 3.5 \times 10^{27}$ erg sec^{-1}	100 %
Converted energy around the X-point		
Electron acceleration around the X-point	$E_{\mathrm{acc}} = 4.0 \times 10^{26}$ erg sec^{-1}	12 %
Thermal heating around the X-point	$E_{\mathrm{th}} = 2.3 \times 10^{26}$ erg sec^{-1}	7 %
Kinetic energy (outflow from the X-point)	$E_{\mathrm{k}} = 1.0 \times 10^{27}$ erg sec^{-1}	30 %
Residual (ion acceleration, wave, etc.)		51 %
Released energy derived from the X-ray emission from the flaring loop		
(Thermal heating + Radiative loss) ×2	$E_{\mathrm{release}} = 2.2 \times 10^{27}$ erg sec^{-1}	64 %

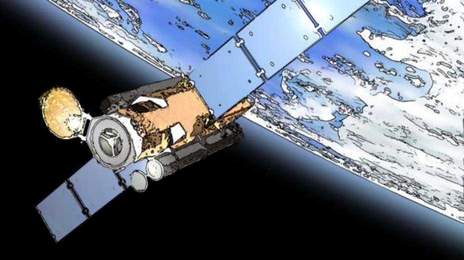

Calibration of NoRH 34GHz data

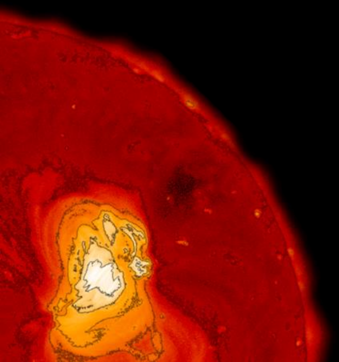

Ghost (Aliasing) pattern appearing in NoRH 34GHz data

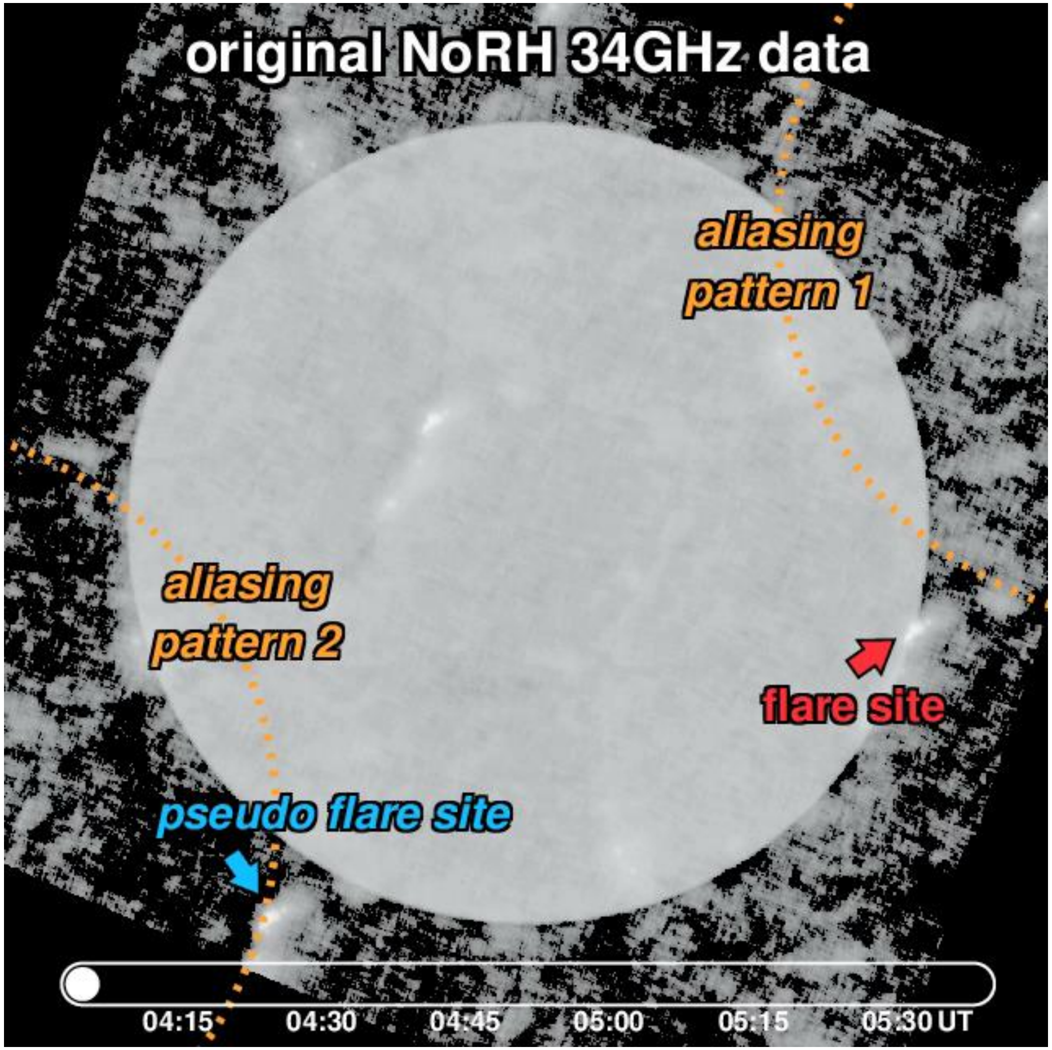

RHESSI 15 - Narukage et al. (2014) ApJ, 787, 125

Detection of ghost (aliasing) pattern

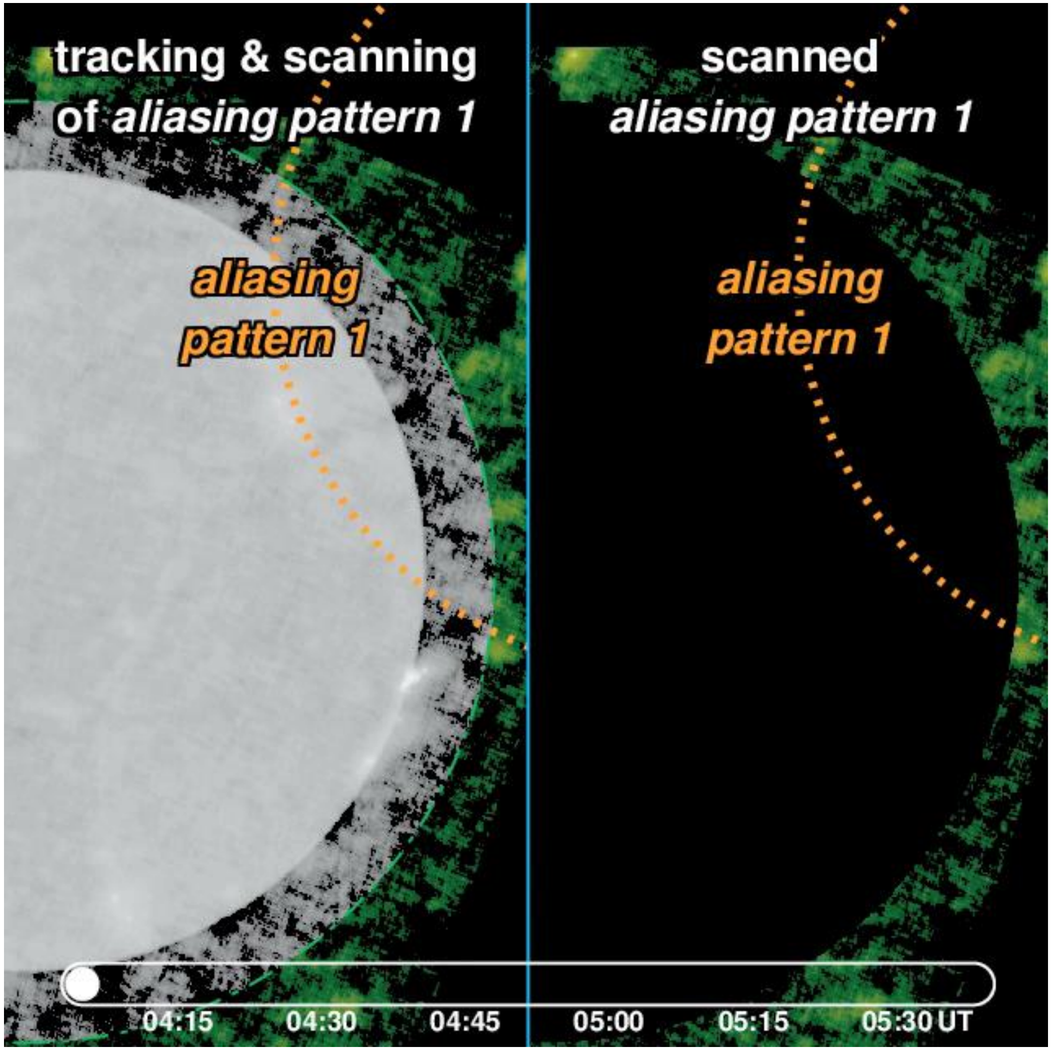

RHESSI 15 - Narukage et al. (2014) ApJ, 787, 125

Calibration results of NoRH 34GHz data

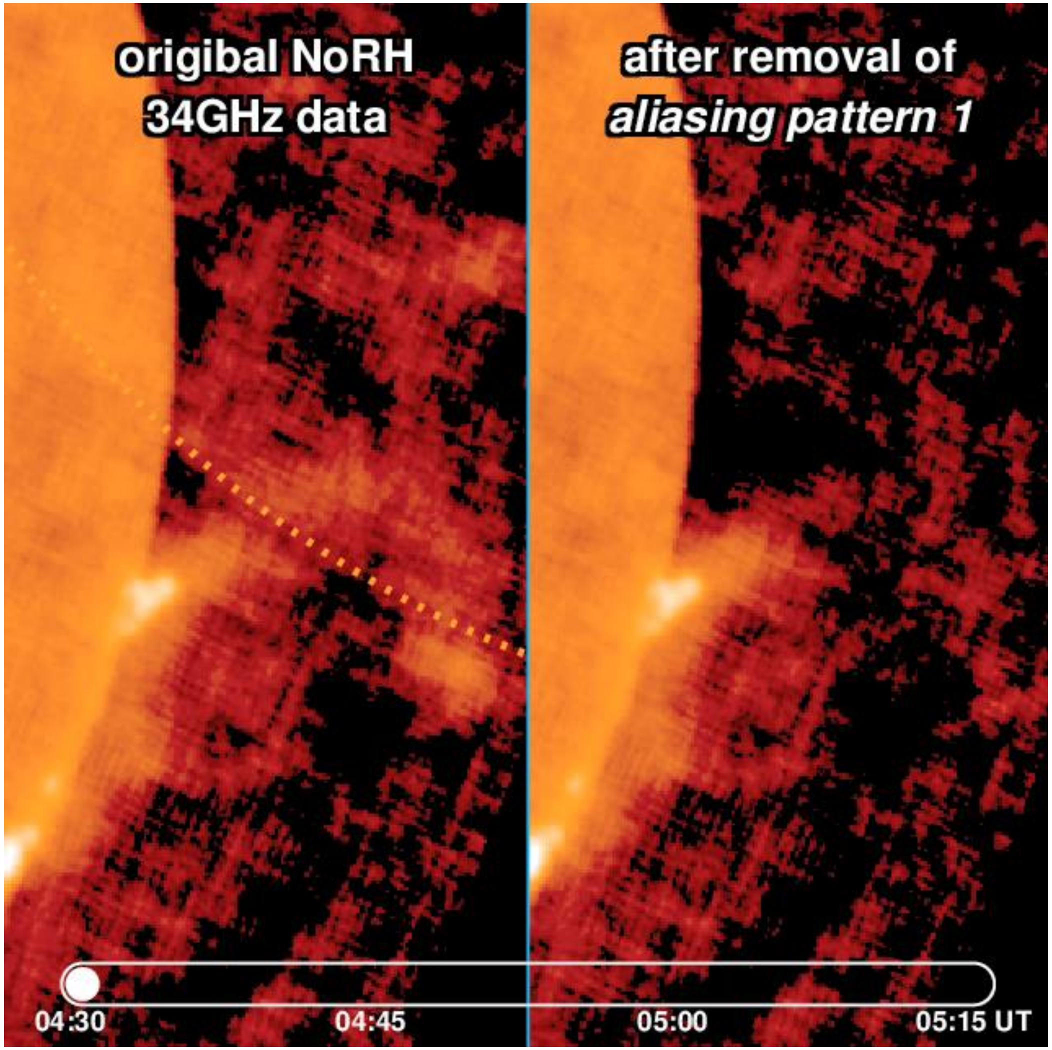

RHESSI 15 - Narukage et al. (2014) ApJ, 787, 125

Error estimate of the calibration result of NoRH 34GHz data

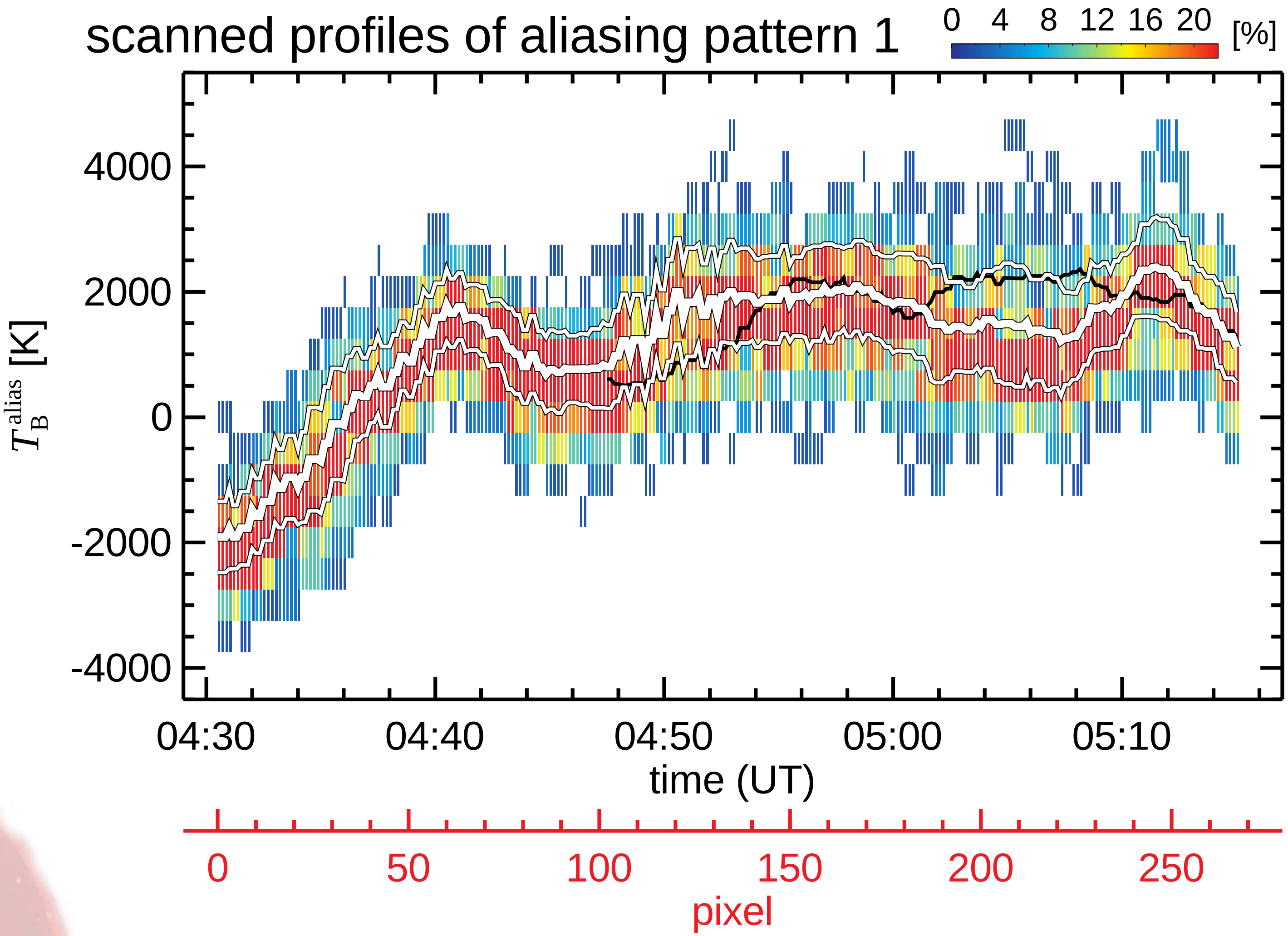

RHESSI 15 - Narukage et al. (2014) ApJ, 787, 125

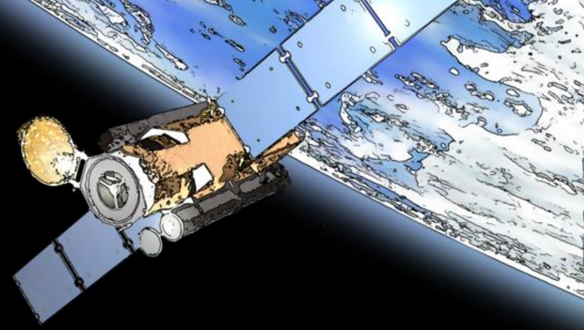

Thank you for your attention.

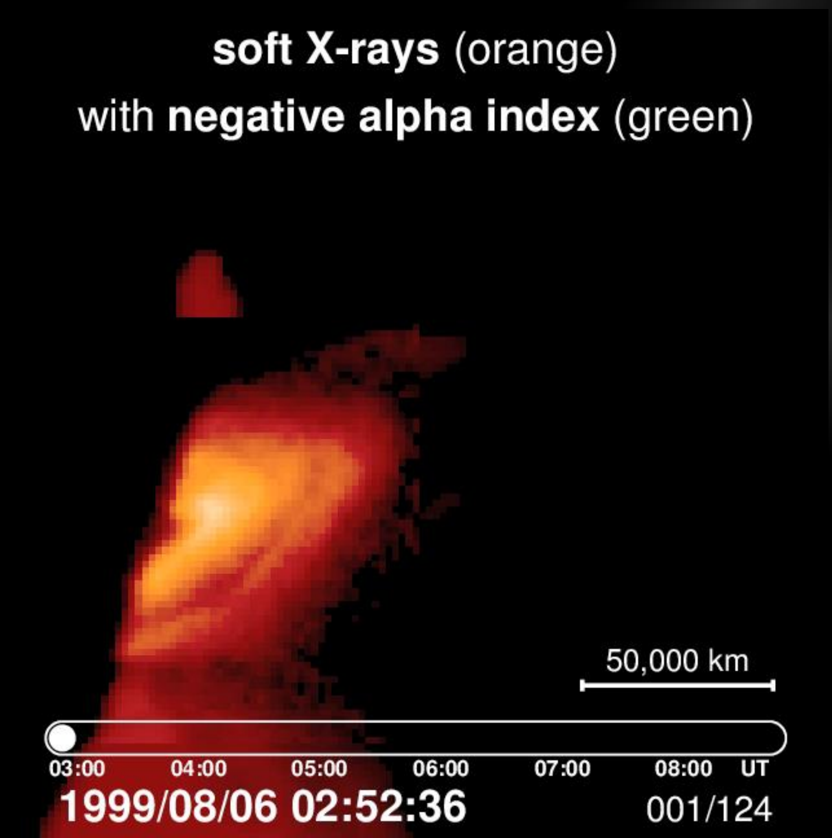

Narukage et al. (2014)
ApJ, 787, 125